Materials Transactions, Vol. 52, No. 3 (2011) pp. 386 to 390

Solidification of High Chromium White Cast Iron Alloyed with Vanadium

Mirjana Filipovic, Zeljko Kamberovic and Marija Korac

Department of Metallurgical Engineering, Faculty of Technology and Metallurgy, University of Belgrade, Karnegijeva 4, 11120 Belgrade, Serbia

Experimental results indicate that vanadium affects the solidification process in high chromium iron. Vanadium is distributed between eutectic M_7C_3 carbide and the matrix, but its content in carbide is considerably higher. Also, this element forms vanadium carbide. TEM observation reveals that vanadium carbide present in examined Fe-Cr-C-V alloys is being of M_6C_5 type. DTA analysis found that with increasing vanadium content in tested alloys, liquidus temperature is decreasing, while eutectic temperature is increasing, i.e. the solidification temperature interval reduces. The narrowing of the solidification temperature interval and the formation of larger amount of vanadium carbides, as a result of the increase in the vanadium content of the alloy, will favour the appearance of a finer structure. In addition, the phases volume fraction will change, i.e. the primary γ-phase fraction will decrease and the amount of M_7C_3 carbide will increase.
[doi:10.2320/matertrans.M2010059]

(Received February 18, 2010; Accepted December 6, 2010; Published February 25, 2011)

Keywords: *vanadium rich carbide, liquidus temperature, eutectic temperature, solidification temperature interval, iron-chromium-carbon-vanadium alloys*

1. Introduction

High chromium white cast irons are an important class of wear resistant materials. Their exceptional wear resistance is the result of their high carbide content, which forms along with austenite during solidification as a proeutectic or eutectic phase depending on alloy composition, and particularly depending upon carbon and chromium content.[1–5)]

The effects of additional alloying elements in high chromium irons have been extensively studied.[6–25)] Normally, alloying additions such as nickel, manganese, molybdenum and copper are used to increase hardenability and to prevent pearlite formation.[2,6)] High chromium irons alloyed with carbide-forming elements such as molybdenum, vanadium and tungsten have been developed for special applications such as hot working mill rolls in the steel industry.[2,12)] Vanadium additions of up to 4 mass% are also said to improve the fracture toughness of both 19% Cr and 27% Cr-3% C irons by refining the eutectic carbide structures.[13,14)] Dupin and Schissler[15)] had previously noted that an addition of 1 mass% V in 20% Cr-2.6% C iron did not produce any vanadium carbide precipitate, but did have a refining effect on the eutectic carbide. Also, A. B. Jacuinde[12)] noticed that an addition of 2 mass% V in 17% Cr-2.6% C iron did not produce any vanadium carbide, but did have increasing volume fraction of M_7C_3 eutectic carbide.

In this work, the influence of vanadium content on the solidification process of high chromium white iron is examined.

2. Experimental Procedure

The chemical composition of tested alloys is listed in Table 1. The melting of various alloys has been conducted in induction furnace. Test samples for structural analysis have been cut from the bars (200 mm long and 30 mm in diameter) cast in the sand molds.

Table 1 Chemical composition of tested Fe-C-Cr-V alloys.

Alloy	Chemical composition (mass%)									
	C	P	S	Si	Mn	Mo	Cu	Ni	Cr	V
1	2.89	0.025	0.061	0.85	0.71	0.48	0.99	0.100	19.03	0.0012
2	2.92	0.025	0.061	0.85	0.75	0.43	1.01	0.098	19.04	1.19
3	2.87	0.024	0.063	0.87	0.73	0.44	1.01	0.099	18.92	2.02
4	2.91	0.027	0.061	0.84	0.73	0.44	1.00	0.096	19.05	3.28
5	2.93	0.026	0.062	0.83	0.74	0.43	1.01	0.098	19.07	4.73

The microstructure was examined using conventional optical microscopy (OM), scanning electron microscopy (SEM) and transmission electron microscopy (TEM). Samples for optical microscope examinations were prepared using standard metallographic technique (etched with picric acid solution (1 g) in methanol (100 ml) by adding 5 ml of hydrochloric acid or etched with Murakami). The size and volume fraction of the phases present in the structure were determined using image analyzer. The morphology of carbide was examined by a scanning electron microscope, JEOL 733-FCXA, using an accelerating voltage of 25 kV. For this examination, the polished samples were deep etched in a 10% HCl solution in methanol for 24 h then cleaned in an ultrasonic bath. The chemical composition of the carbides was determined using energy dispersive X-ray spectroscopy (EDS). Discs for TEM examinations were prepared by using a twin-jet electropolisher. These samples were examined at 200 kV in a JEOL-2000FX transmission electron microscope.

The phase transformations during solidification of the examined alloys were controlled by differential thermal analysis (DTA) method. For this examination a Du Pont 1090B analyzer was used with a high temperature cell, 1600DTA. The temperature difference of the examined and reference sample was recorded during cooling at a rate of $5^{\circ}C\,min^{-1}$, within temperature interval 1000–1480°C, in a helium protective atmosphere.

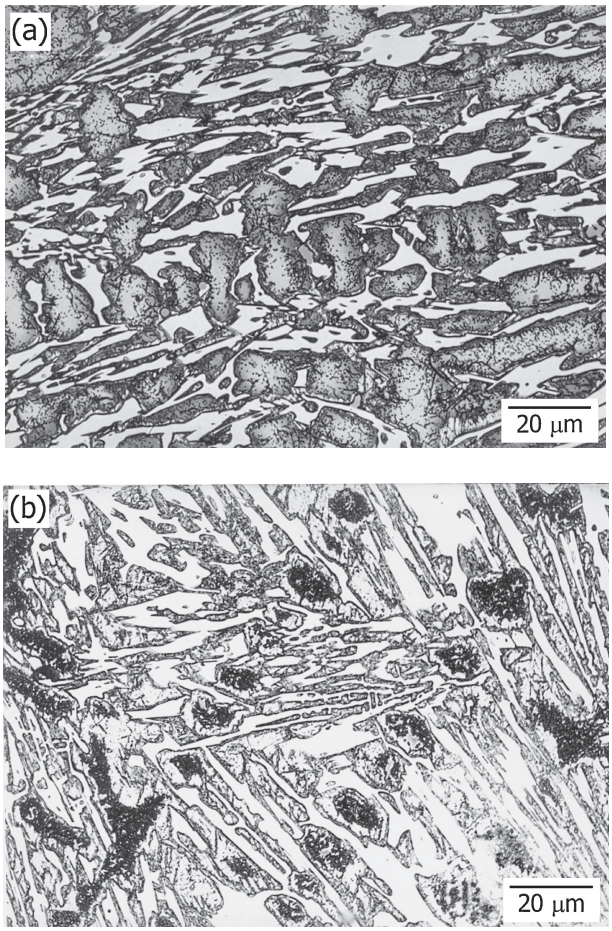

Fig. 1 Optical micrographs of Fe-Cr-C-V alloy containing: (a) 1.19% V (b), 3.28% V.

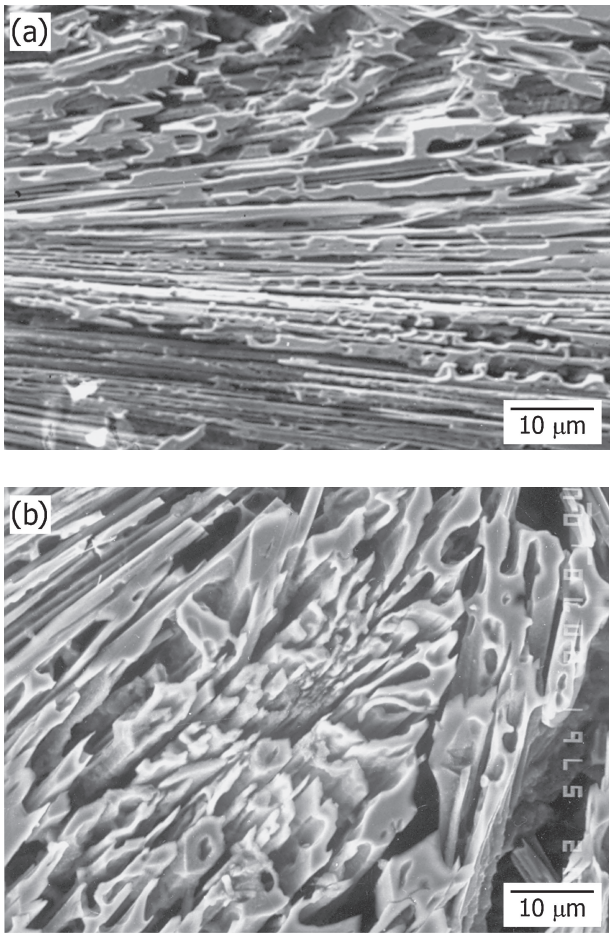

Fig. 2 SEM micrographs of deep etched sample showing morphology of M_7C_3 carbides in Fe-Cr-C-V type alloy containing 3.28% V: (a) eutectic colonies consisting of a larger number of long M_7C_3 carbide rods which grow along their longitudinal axes; (b) eutectic colonies when viewed perpendicular to their fastest growth direction (mainly composed of very fine rode-like carbides in the center, becoming coarser rod-like or blade-like with increased distance from the centre).

3. Results

The as-cast microstructure of examined alloys contain primary austenite dendrites and eutectic colonies composed of M_7C_3 carbides and austenite (Fig. 1).

The SEM micrographs of deep etched sample revealed that single M_7C_3 carbides in all tested Fe-Cr-C-V alloys were rod or blade shaped (Fig. 2), where the blades are basically consist of multiple rods (Fig. 2(b)). A larger number of long carbide rods within the eutectic colonies usually grow along their longitudinal axes (Fig. 2(a)). When viewed perpendicular to their fastest growth direction, the M_7C_3 carbides within the eutectic colonies are very fine rod-like at the center, but become coarser rod-like or blade-like (Fig. 2(b)) with increasing distance from the center.

When the reagent for selective etching of carbide was used (whereby the M_7C_3 carbide become dark brown and vanadium carbide white), fine, white particles were noticed in the structure of alloy containing 1.19% V (Fig. 3).

Figure 4(b) shows not only that the vanadium is distributed between eutectic M_7C_3 carbide and the matrix and that its content in carbide is considerably higher, but also the area of high vanadium concentration, corresponding to particle marked C from Fig. 4(a).

Vanadium carbide has nearly spherical shape (Fig. 5(a)). EDS analysis (Fig. 5(b)) indicates that this carbide

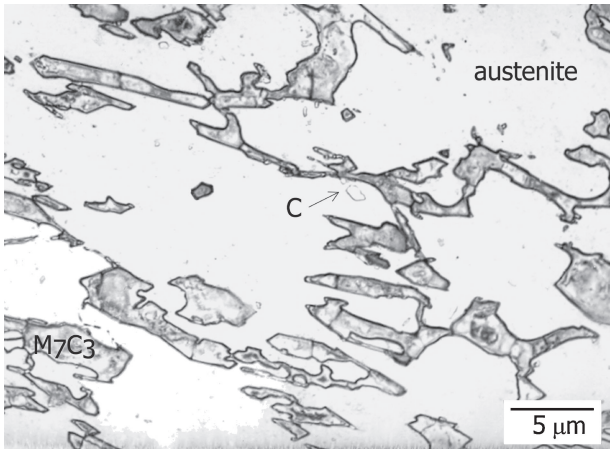

Fig. 3 Optical micrographs of Fe-Cr-C-V alloy containing 1.19% V (etched with Murakami).

(Fig. 5(a)) contains 50.86 mass% V, 15.94 mass% Cr i 15.73 mass% Fe.

Vanadium carbide present in examined Fe-Cr-C-V alloys was identified as M_6C_5 type carbide (Fig. 6). Stacking fault is clearly visible within the carbide (Fig. 6).

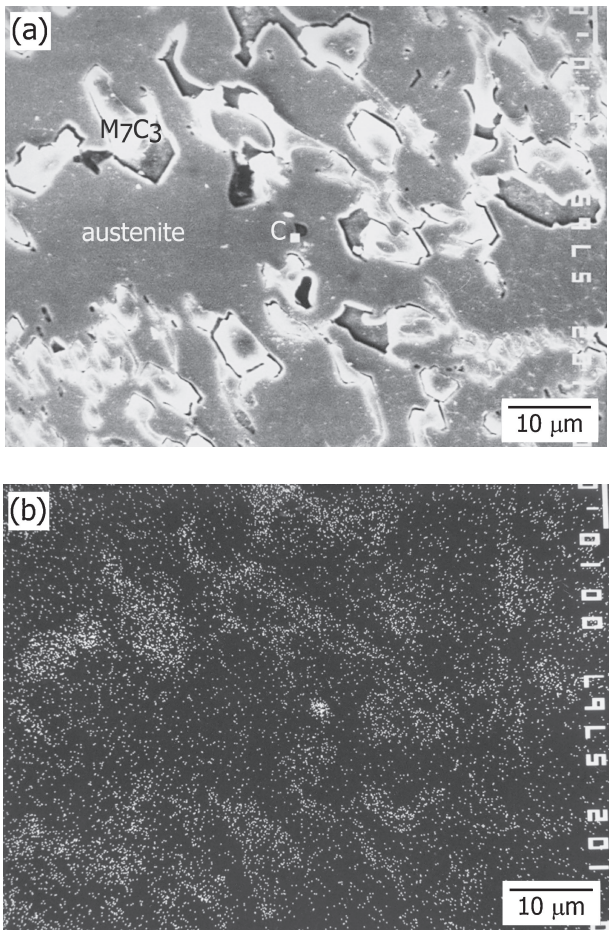

Fig. 4 SEM micrograph of as-cast microstructure in Fe-Cr-C-V alloy containing 1.19% V (a) and corresponding vanadium distribution map (b).

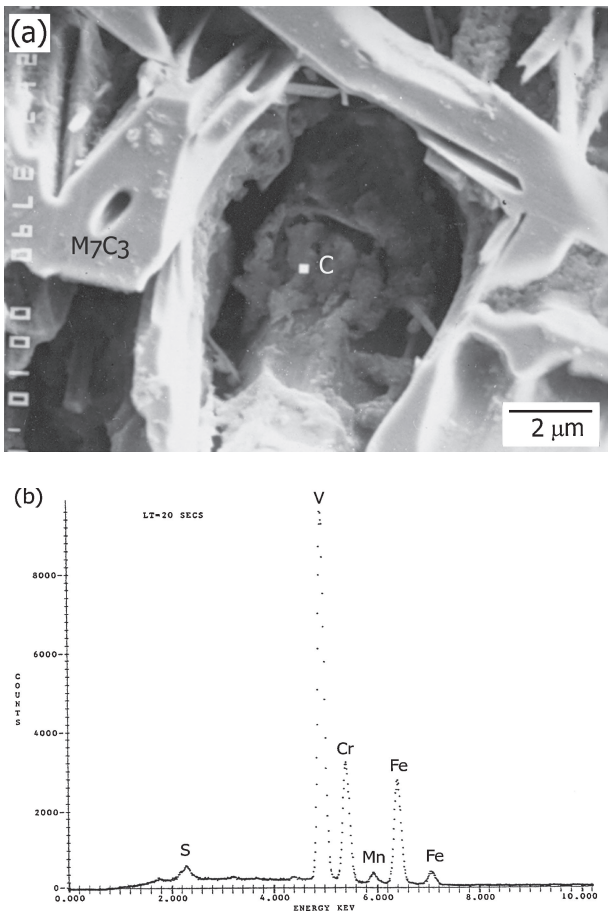

Fig. 5 SEM micrographs of deep etched sample showing morphology of vanadium carbide (a) and EDS spectrum of this carbide (b) in Fe-Cr-C-V alloy containing 1.19% V.

Table 2 and Fig. 7 show the results obtained by DTA analysis. With increasing vanadium content in tested alloys, liquidus temperature is decreasing, while eutectic temperature is increasing, i.e. the solidification temperature interval reduces.

The volume fraction and size of phases in the microstructure of the examined alloys are shown in Table 3. With increasing vanadium content in the alloy, the volume fraction of primary austenite is decreased, whereas the amount of M_7C_3 and M_6C_5 carbides are increased. In adition, dendrite arms spacing (DAS) and size of eutectic M_7C_3 carbides are decreased, while the size of M_6C_5 carbides is increased with increasing vanadium content.

The cooling rate of tested samples cast in sand molds was determined by using the equation:[26,27)]

$$d = B \cdot (V_h)^{-n}$$

where is d—the dentrite arms specing, μm; V_h—the cooling rate, °C/s; B and n—constants.

According to litterature,[27)] constant B which depends on alloy composition is ranging between 14.6 and 30.2 μm s/°C for alloys with high chromium content. For examined Fe-C-Cr-V alloys 14.6 μm s/°C the adopted value is B. The constant n values are in the interval of $1/2 - 1/3$, the recomended value for this alloys type being $n = 1/3$. The calculated cooling rate of tested samples is approximately $1\,^{\circ}C\,s^{-1}$.

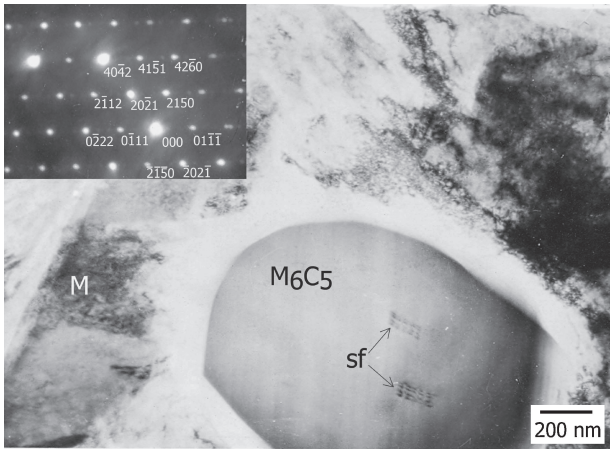

Fig. 6 Transmission electron micrograph of the Fe-Cr-C-V alloy containing 1.19% V showing vanadium carbide and selected-area diffraction pattern (in the corner) from the region in this micrograph, (markings on the micrographs: sf-stacking fault, M-martensite).

4. Discussion

Experimental results indicate that vanadium affects the solidification process in high chromium white cast irons. With an increase of vanadium content the alloy composition approaches the eutectic composition in quaternary Fe-Cr-C-

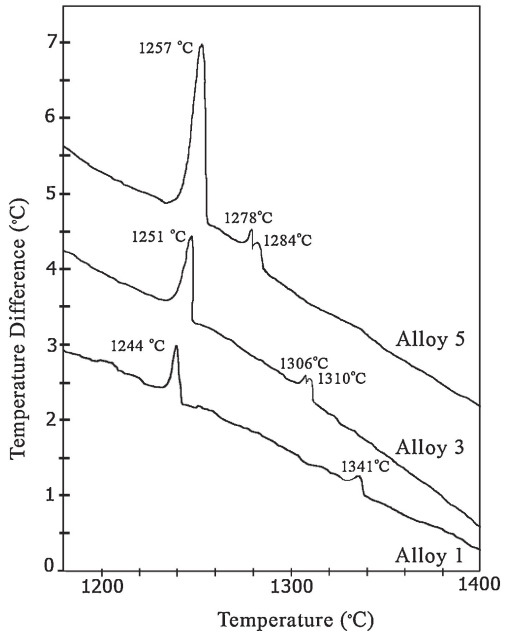

Fig. 7 DTA curves for the alloys 1, 3 and 5 obtained at a cooling rate of $5^{\circ}C\,min^{-1}$.

Table 2 DTA results of the examined Fe-Cr-C-V alloys.

Alloy	V in alloy (mass%)	Temperature (°C)			
		T_L	$T_{E_1(V_6C_5+\gamma)}$	$T_{E(M_7C_3+\gamma)}$	ΔT
1	—	1341	—	1244	97
2	1.19	1319	1315	1249	70
3	2.02	1310	1306	1251	59
4	3.28	1299	1294	1254	45
5	4.73	1284	1278	1257	27

T_L-the start temperature of the austenite reaction (liquidus); $T_{E_1(V_6C_5+\gamma)}$-the temperature of the eutectic reaction $E_1(L \rightarrow V_6C_5 + \gamma)$; $T_{E(M_7C_3+\gamma)}$-the temperature of the eutectic reaction $E(L \rightarrow M_7C_3 + \gamma)$; ΔT-the solidification temperature interval.

Table 3 The volume fraction and size of phases in the microstructure of the examined Fe-Cr-C-V alloys.

Alloy	V in alloy (mass%)	Volume fraction (vol%)			Size (μm)		
		primary γ-Fe	M_7C_3	M_6C_5	DAS	M_7C_3	M_6C_5
1	—	50.83	30.97	—	14.08	7.48	—
2	1.19	47.48	31.96	1.58	12.76	6.74	1.26
3	2.02	45.76	32.82	2.31	11.93	6.52	1.31
4	3.28	42.05	34.31	3.12	10.67	5.67	1.45
5	4.73	39.15	35.47	4.27	9.45	5.03	1.52

V system, causing a decrease of the solidification temperature interval (Table 2 and Fig. 7).

Solidification starts with formation of γ-phase at 1341°C in Fe-Cr-C alloy with no vanadium addition, at 1319°C in Fe-Cr-C-V alloy containing 1.19% V, and at 1284°C in Fe-Cr-C-V alloy containing 4.73% V. In the course of primary γ-phase growth, the composition of the remained liquid was changing. Due to limited solubility of carbon, chromium and vanadium in the austenite, these elements accumulated in front of the progressing solid-liquid interface. At temperatures little bit lower than liquidus temperature (1315°C in alloy containing 1.19% V, 1278°C in alloy containing 4.73% V) during the eutectic reaction that takes place, in local areas enriched in vanadium, eutectic composed of vanadium rich carbide and austenite was developed. Particles of vanadium carbides disturb or completely block further γ-phase growth, with the efficiency depending on their volume fraction, size and distribution.

As the temperature falls and solidification progresses, primary austenite dendrites reject solute (carbon, chromium and vanadium) in to the remaining liquid until the eutectic composition is reached and the monovariant eutectic reaction ($L \rightarrow \gamma + M_7C_3$) takes place. From the melt remained in interdendritic regions the coupled austenite-M_7C_3 eutectic was forming at 1244°C in Fe-Cr-C alloy with no vanadium adition, at 1249°C in alloy containing 1.19% vanadium, and at 1257°C in alloy containing 4.73% vanadium. The eutectic regions of carbide and austenite grow as colonies, indicating growth of a faceted-nonfaceted eutectic. A. Bedolla-Jacuinde *et al.*[4] found that M_7C_3 eutectic carbides in high chromium white irons nucleated on the surface of the primary and secondary dendrites arms. The eutectic γ-phase nucleated side-by-side with the hexagonal M_7C_3 carbides, and both eutectic constituents may then grow more or less at the same rate with bars surrounded by austenite, and coupled growth develops. During eutectic growth, the solute atoms (chromium, vanadium and carbon), which are rejected by one phase, are usually needed for the growth of the other.

Morphology of eutectic colonies depended mainly on the amount and shape of austenite dendrites.

The eutectic carbides are usually aligned so that the long axis of the carbide rods is parallel with the direction of heat flow (i.e. perpendicular to the cast surface). The morphology of the eutectic carbides varied from the center to the edge of a eutectic colony in all examined alloys. The rod shaped carbides are finer at the center of the eutectic colony and become coarser rod-like or blade-like with increased distance from the center (Fig. 2(b)), as indicates that eutectic solidification begins at the center with a certain bulk undercooling and proceeds radially outward. As solidification progresses, the undercooling decreases, and thus the rod-like or blade-like carbides that form during the later stages of solidification are coarser. These results agree with those of K. Ogi[23] and Ö. N. Doğan *et al.*,[1] who found that the undercooling decreases in the course of the eutectic colony's growth, due to latent heat released during solidification.

The main phase transformations observed by DTA analysis during cooling at a rate of $5^{\circ}C\,min^{-1}$ also occur when a melt of similar composition is poured into a sand mold during cooling at a rate of $60^{\circ}C\,min^{-1}$.

TEM observation reveals that vanadium carbide present in examined Fe-Cr-C-V alloys is being of M_6C_5 type (Fig. 6). The same type of carbide was found by J. D. B. De Mello *et al.*[20] in cast iron containing 10% Cr and 6% V.

The results presented in this work show that vanadium rich carbides were formed in alloy containing 1.19% V (Figs. 3–7, Table 2). P. Dupin and J. M. Schissler[15] did not detect the vanadium carbide formation in high chromium white cast iron with 1% V. Nonetheless, A. Bedolla-Jacuinde *et al.*[12] in

16.9% Cr-2.58% C-1.98% V alloy and Y. Matsubara *et al.*[24] in 17.54% Cr-3.57% C-3.14% V alloy observed that (γ + MC) eutectic solidification did not occur because of lower vanadium content, which was different from the report of M. Stefanescu and S. Cracium[22] who indicated that vanadium carbides are present in the microstructure of 14.66% Cr-2.95% C-2.9% V alloy. Furthermore, Sawamoto *et al.*[7] found that vanadium carbides are forming in high chromium white cast irons containing more than 5% V. The established disagreement appears to be a result of different cooling conditions, on one hand, and of the fact that vanadium carbides are difficult to notice due to their small volume fraction and size, on the other hand.

When the solidification temperature interval is narrower (as the consequence, in this case, of alloying high chromium white iron with vanadium), around the primary dendrite of the γ-phase in the remaining portion of the melt, the temperature and concentration conditions appear more readily, thus enabling the formation of eutectic colony nuclei and their growth which results in the interpretation of further γ-phase growth. The eutectic colonies growth rate well increase with increasing eutectic temperature, i.e. with a lowering of the solidification temperature interval, thus influencing the formation of a larger amount of finer M_7C_3 carbides (Table 3).

5. Conclusions

The microstructure of examined Fe-Cr-C-V alloys consists of M_7C_3 and vanadium rich M_6C_5 carbides in austenitic matrix.

Vanadium affects the solidification process in high chromium irons. With an increase of vanadium content the alloy composition approaches the eutectic composition in the quaternary Fe-Cr-C-V system, causing a decrease of the solidification temperature interval, and thereby also changing the volume fraction, size and morphology of the present phases.

In the process of cooling at the same rate, the narrowing of the solidification temperature interval and the formation of larger amount of vanadium carbides, as a result of the increase in the vanadium content of the alloy, will favour the appearance of a finer structure which is manifested by the reduced width of dendrite arms and the reduced size of eutectic M_7C_3 carbide. In addition, the phases volume fraction will change, i.e. the primary γ-phase fraction will decrease and the amount of M_7C_3 carbide will increase.

REFERENCES

1) Ö. N. Doğan, J. A. Hawk and G. Laird II: Metall. Mater. Trans. **28A** (1997) 1315–1328.
2) C. P. Tabrett, I. R. Sare and M. R. Ghomashchi: Int. Mater. Rev. **41** (1996) 59–82.
3) Ö. N. Doğan: Scr. Mater. **35** (1996) 163–168.
4) A. Bedolla-Jacuinde, B. Hernández and L. Béjar-Gómez: Z. Metallkd. **96** (2005) 1380–1385.
5) G. Laird II and Ö. N. Doğan: Int. J. Cast Metals Res. **9** (1996) 83–102.
6) Z. Sun, R. Zuo, C. Li, B. Shen, J. Yan and S. Huang: Mater. Charact. **53** (2004) 403–409.
7) A. Sawamoto, K. Ogi and K. Matsuda: AFS Trans. **94** (1986) 403–416.
8) C. R. Loper and H. K. Baik: AFS Trans. **97** (1989) 1001–1008.
9) A. Sawamoto, K. Ogi and K. Matsuda: J. Jpn. Inst. Met. **49** (1985) 475–482.
10) H. K. Baik and C. R. Loper: AFS Trans. **96** (1988) 405–412.
11) M. Fiset, K. Peev and M. Radulovic: J. Mater. Sci. Lett. **12** (1993) 615–617.
12) A. Bedolla-Jacuinde: Int. J. Cast Metals Res. **13** (2001) 343–361.
13) M. Radulovic, M. Fiset, K. Peev and M. Tomovic: J. Mater. Sci. **29** (1994) 5085–5094.
14) B. M. Hebbar and S. Seshan: AFS Trans. **92** (1984) 349–354.
15) P. Dupin and J. M. Schissler: AFS Trans. **92** (1984) 355–360.
16) A. Wiengmoon, T. Chairuangsri, A. Brown, R. Brydson, D. V. Edmonds and J. T. H. Pearce: Acta Mater. **53** (2005) 4143–4154.
17) J. Wang, R. L. Zuo, Z. P. Sun, C. Li, K. K. Liu, H. S. Yang, B. L. Shen and S. J. Huang: Mater. Charact. **55** (2005) 234–240.
18) A. Bedolla-Jacuinde, R. Correa, J. G. Quezada and C. Maldonado: Mater. Sci. Eng. A **398** (2005) 297–308.
19) H. Fushend and W. Chaochang: J. Mater. Sci. Techol. **5** (1989) 918–924.
20) J. D. B. De Mello, M. Durand-Charre and T. Mathia: Mater. Sci. Eng. **78** (1986) 127–134.
21) M. Filipovic, E. Romhanji, Z. Kamberovic and M. Korac: Mater. Trans. **50** (2009) 2488–2492.
22) D. M. Stefanescu and S. Cracium: Fonderie **32** (1977) 51–60.
23) K. Ogi, Y. Matsubara and K. Matsuda: AFS Trans. **89** (1981) 107–204.
24) Y. Matsubara, N. Sasaguri, K. Shimizu and S. K. Yu: Wear **250** (2001) 502–510.
25) W. M. Zhao, Z. X. Liu, Z. L. Ju, B. Liao and X. G. Chen: Mater. Sci. Forum **575–578** (2008) 1414–1419.
26) H. F. Fischmeister, R. Riedl and S. Karagoz: Metall. Mater. Trans. **20** (1989) 2133–2147.
27) Y. K. Jang and F. Jeglitsch: Z. Metallkd. **76** (1985) 717–723.